Elektronica en Telecommunicatie 7

Gemeenschappelijke publikatie van de
Sectie voor Telecommunicatietechniek van het K.I.v.I. en het
Nederlands Elektronica- en Radiogenootschap.
Redactie-adres: Prinsessegracht 23, Den Haag.

621.396.962

RUDAR – An experimental Noise Radar System

by ir. J. A. Smit and W. B. S. M. Kneefel, Christiaan Huygenslaboratorium, Noordwijk

Synopsis: The results of experiments with a noise radar, performed in 1964, are given. Attention has been focussed on a flexible cross-section of a possible complete system. As a consequence of this we were able to check the system performance in a straightforward manner with relatively simple hardware. Several features of the system have been shown, viz.:
- the antenna system can be used as a space filter;
- there is an option for azimuth measurement by mechanical or frequency-scanning.

A discussion will be given of the advantages and disadvantages of such a system.

1. Introduction

In the available literature several references can be found quoting noise as a possible radar signal source [1, 2, 3, 4, 5]. However, *application* of this type of signal *in a system* has, as far as we know, only been mentioned by a few authors [6, 7, 8, 9]. For this reason it may be of interest to give the results of our experiments with a noise radar obtained in 1964.

Prior to the actual experiment in question we did some work on microwave correlators for measuring purposes. As an example a *noise-reflectometer-system* could be mentioned. In fact it is a radar-system for short distances but with a high resolution (about 30 cm) and a high accuracy in target-distances (about 1 cm) and target strength (about 5%). In Fig. 1 an example is given of a measurement [10].

Our further research was directed to the use of frequency-dispersive antennas as a means to spread the available frequency spectrum in space. For, when a broadband signal (e.g.

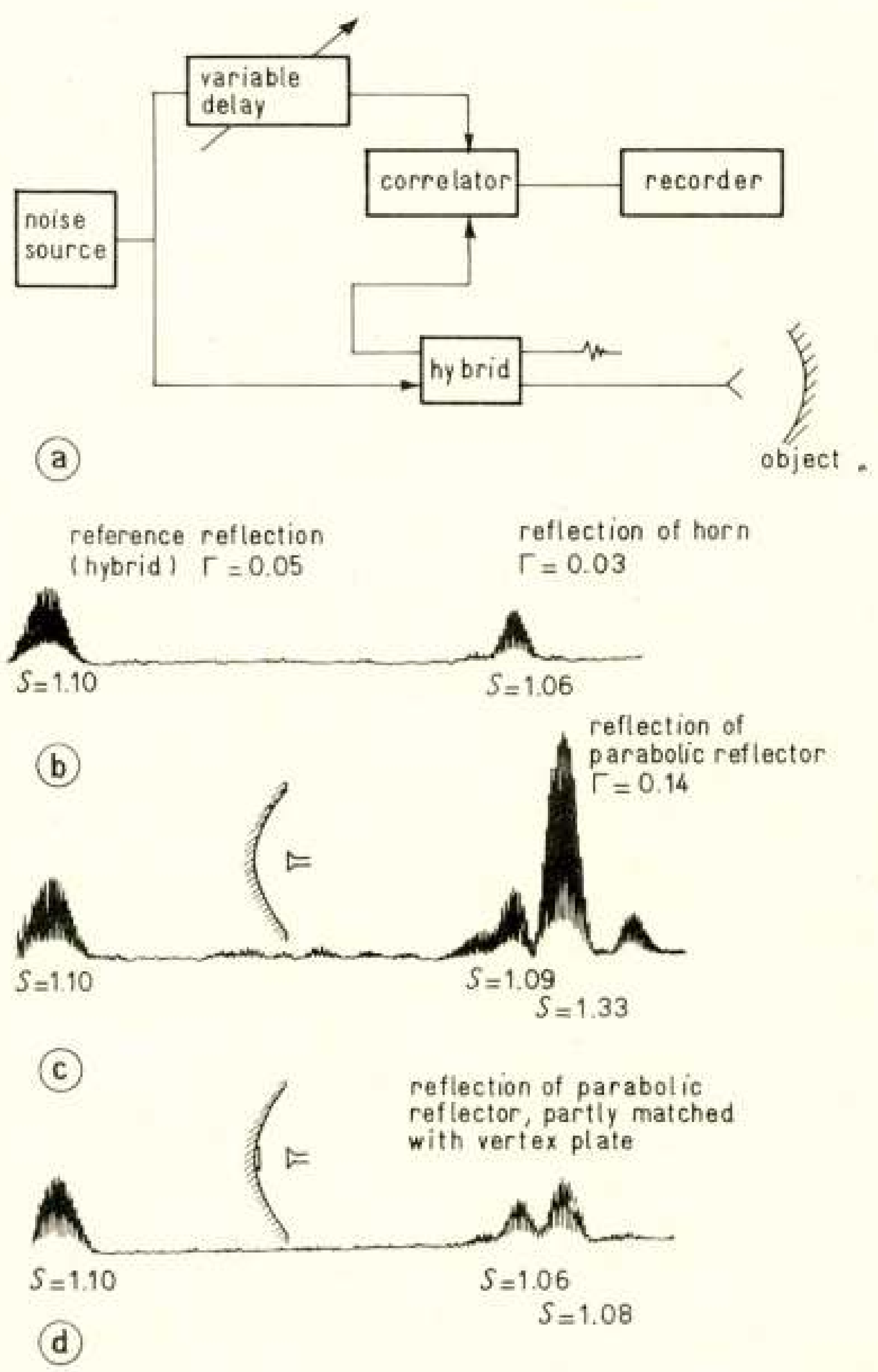


Fig. 1. Example of measurement with a microwave noise-reflectometer system: matching of a parabolic reflector at 9000 MHz; spectrum bandwidth: 1000 MHz.

a. Block diagram of reflectometer. b. Correlator output signal for cross-coupling of hybrid (reference) reflection and reflection of horn (S = V, S, W, R). c. Correlator output signal, as in b., and horn placed in focal point of a parabolic reflector. d. Correlator output signal, as in c., parabolic reflector provided with a 'vertex plate'.

N.a.v. een 'paper' ingezonden naar de AGARD Conference on Advanced Radar Systems, Istanbul, mei 1970.

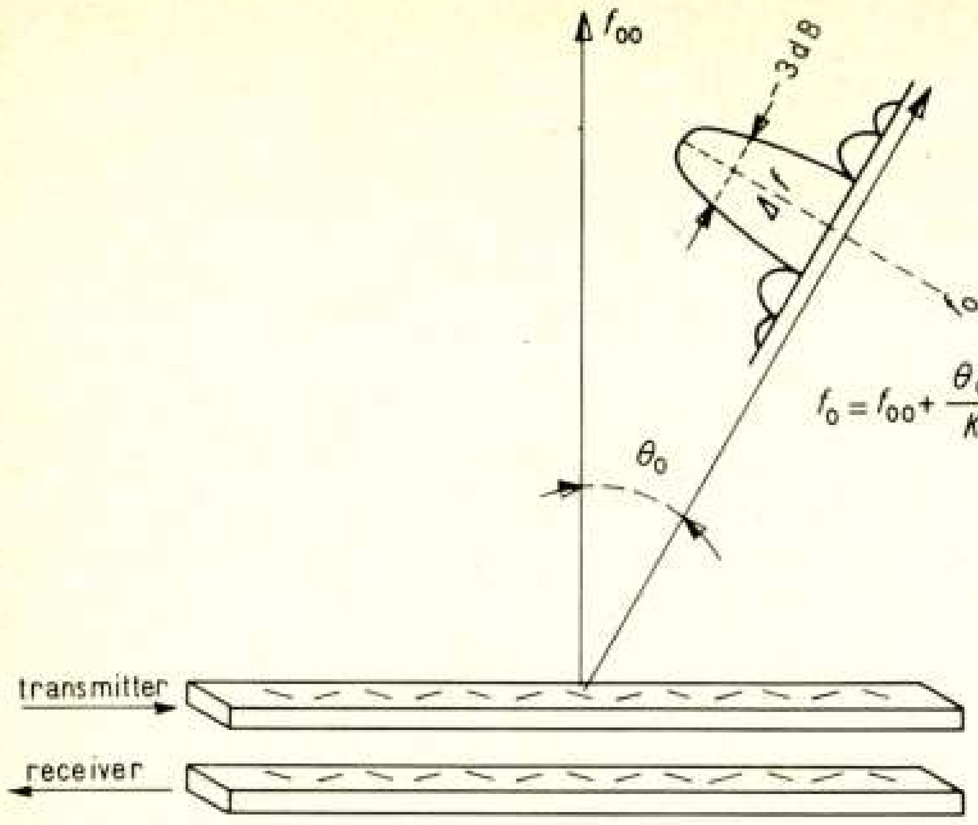


Fig. 2. Linear array as a space filter.

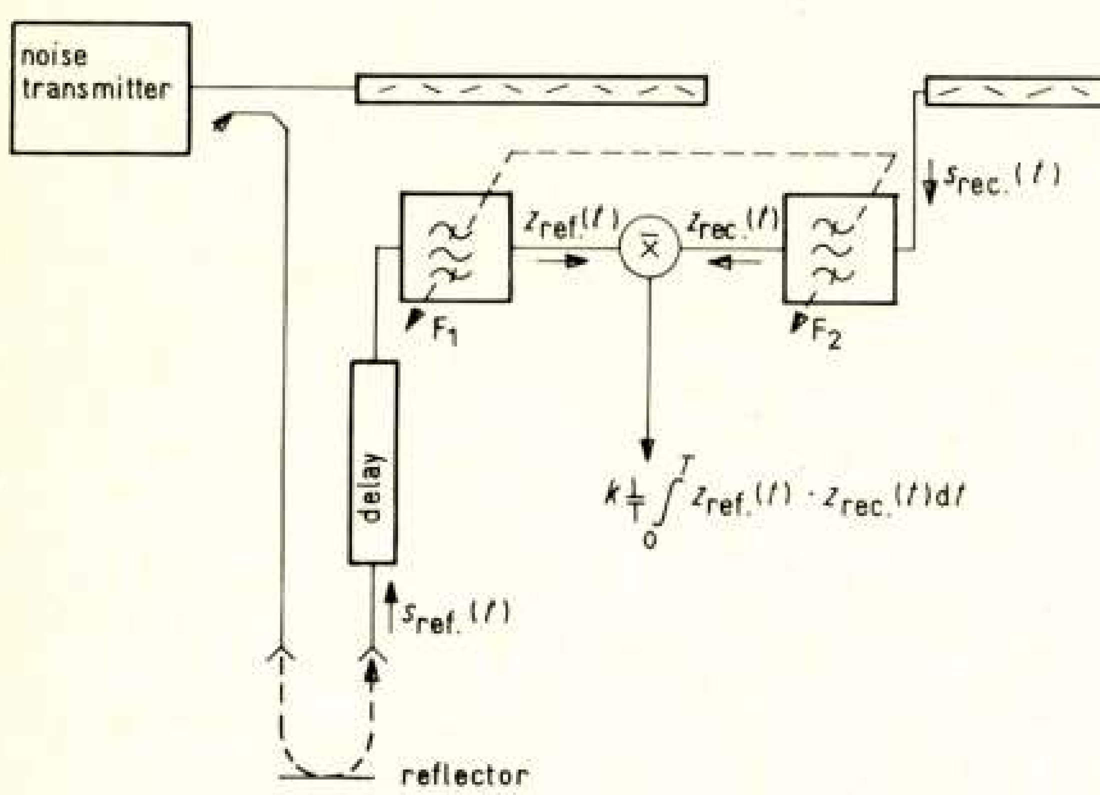


Fig. 3. Block diagram of a noise radar.

a noise signal) is transmitted by an end-fed linear array, the spectrum of this signal will be spread out in space owing to the antenna 'squint' (Fig. 2).

In a direction θ, in the far field, the spectrum received will have a center frequency specified by the direction θ and a form specified by the antenna pattern. The bandwidth of this spectrum with an antenna beamwidth of $\theta^{\circ}_{-3\,dB}$, and a squint-factor of K°/MHz, will be: $B = \theta_{-3\,dB}/K$ (MHz).

For detection of a signal that has been reflected by an object in a direction θ, the receiver should be matched to the signal:

a. *in the frequency domain,*
with a filter, with center frequency f_0 and a form dependent on the beam pattern;

b. *in the time domain,*
with a correlator, because we are dealing with a noise signal.

The block diagram of the noise radar with a dispersive system will be as given in Fig. 3. In the ideal case a precise distance measurement can theoretically be done by means of the maximum of the fine structure. But as result of fluctuations in electromagnetic propagation and target motion, the delay time τ is subject to variations. Therefore an envelope correlator detector is required. Three possible configurations for envelope correlators are given in Fig. 4a ... c. In the Appendix 7.1. more details of these circuits are to be found.

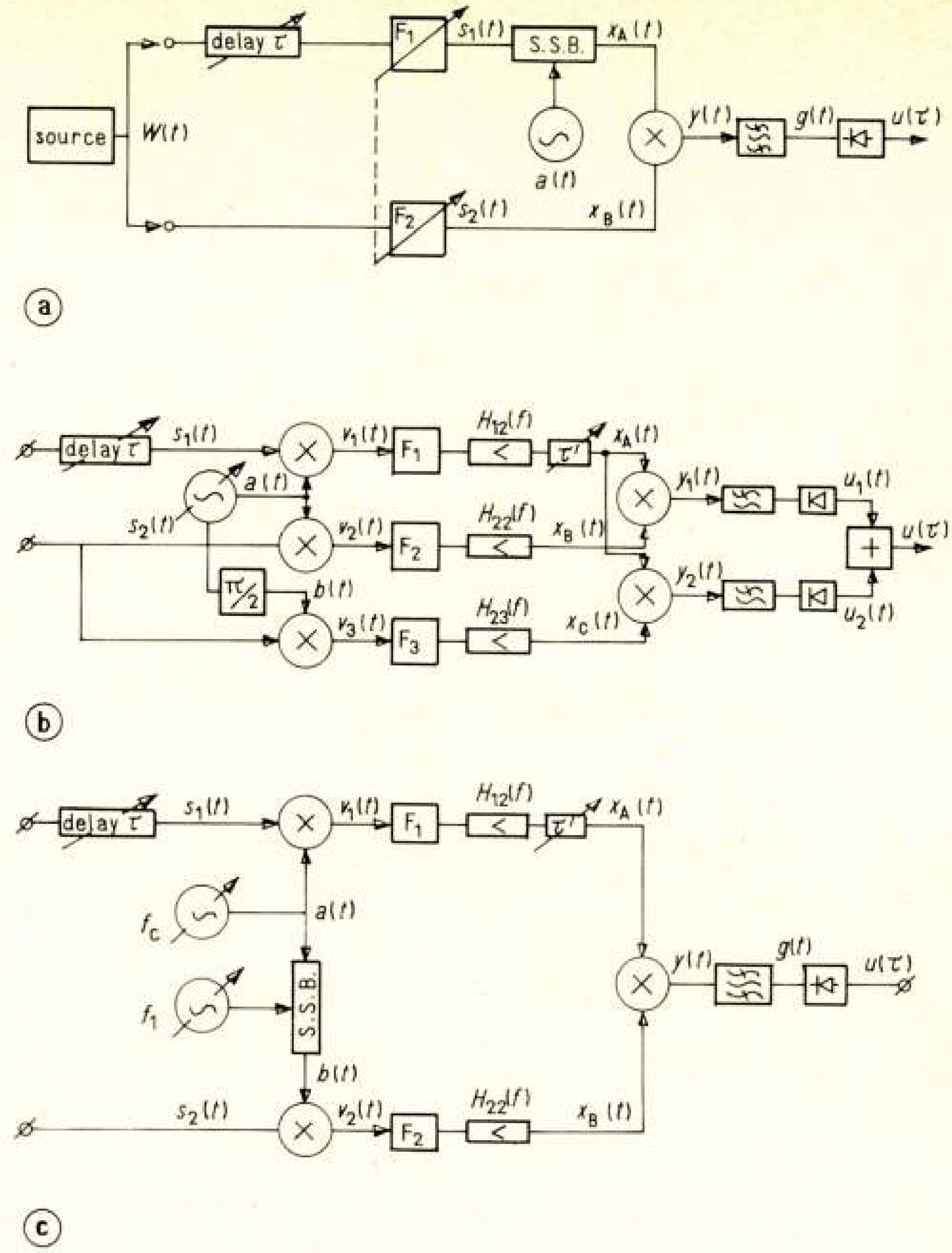


Fig. 4. Microwave envelope-correlator configurations.

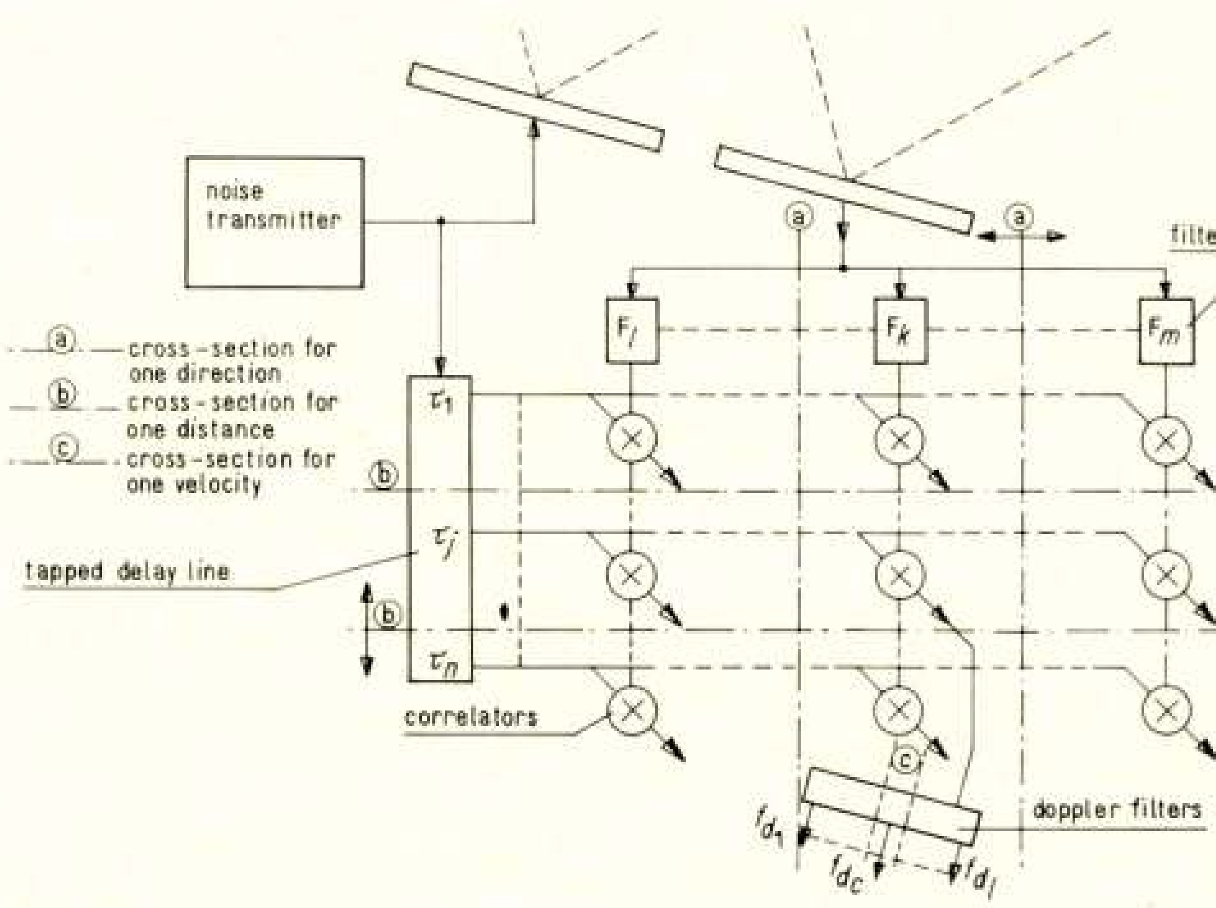


Fig. 5. Block diagram of complete noise radar system.

2. The scope of the experiment

The objective of the experiment was to investigate a complete noise-radar system, making a cross-section of the system. In Fig. 5 a block diagram of a complete system is given. Target

bearing is measured by means of the filters F_1 ... F_m, target range by means of the delays τ_1 ... τ_n, while target velocity is measured by means of the doppler shift f_d, in filters f_{d1} to f_{dl}. The observed space is divided in $n \times m$ space-cells, and each cell will be divided in l doppler slots.

A cross-section as mentioned can be given either by:

a. one direction, given by F_k, and n delay steps, with n correlators and $n \times l$ doppler filters;

b. one distance, given by τ_j, and m bearing filters, with m correlators and $m \times l$ doppler filters;

c. one direction, given by F_k, and one distance, given by τ_j, with one correlator and one doppler slot, f_{di}.

If in the third alternative F_k, τ_j and f_{di} are made variable, a good impression of the behaviour of a complete system may be obtained. The scope of an experiment with such a flexible set-up is:

a. *to test the principle of noise radar*
 - a. 1. Is it in fact possible to detect a target in very poor S/N-conditions?
 - a. 2. Can a dispersive linear array be used as a space filter?
 - a. 3. Is it possible to resolve targets with different speeds in the same space-cell?
 - a. 4. What is the optimum bandwidth of the bearing filters?
 - a. 5. Is it allowed to extrapolate the results of one space-cell to a system with $n \times m \times l$ facets?

b. *to discover the drawbacks*
 - b. 1. the detrimental effect of the cross-coupling between transmitter- and receiver-antenna;
 - b. 2. the influence of nearby targets;
 - b. 3. the effects of spurious signals in the delay line.

c. *measurements*
 - c. 1. target position and velocity;
 - c. 2. cross-correlation function;
 - c. 3. antenna squint characteristics.

3. The system

3.1. *System requirements*

Another objective of the experiment was to verify the expected theoretical relations of the various parameters. Therefore it is of little use to specify in advance center frequencies, bandwidth, etc. As a consequence of this, it was decided:

- that the maximum bandwidth of the receivers should not be limited by the choice of the delay line;
- to construct one filter-correlator combination, with the requirement that the center frequency and the bandwidth of the filter must be variable;
- to obtain the *speed information* from the fluctuation rate of the fine-structure of the correlation function.

From the requirements just stated, the principle of the system can be given. The method given in Fig. 4c is most suitable. The reasons for this are the following:

- there are no image frequencies;
- the video-bandwidth can be half the R.F.-bandwidth.

The video amplifiers (filters F_1 and F_2) are not made as real low-pass filters, but a cut-off frequency $> f_1$ is given for the lower frequencies.

Then signals with a frequency f_1 are suppressed; these are produced at:

- the S.S.B.-modulator, by crosstalk;
- the mixer, as a consequence of unbalanced amplitude modulation.

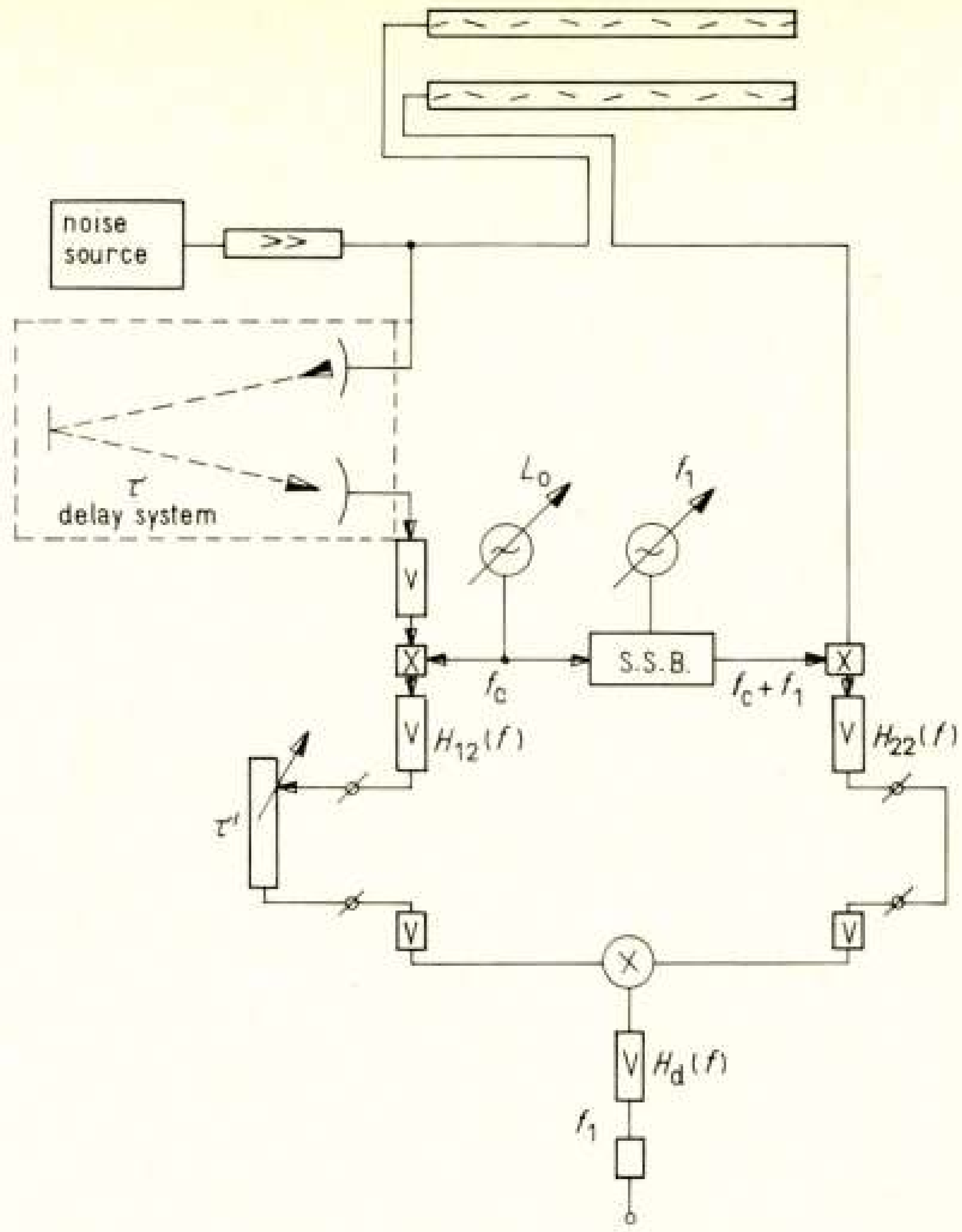


Fig. 6a. Block diagram of realized RUDAR-system.

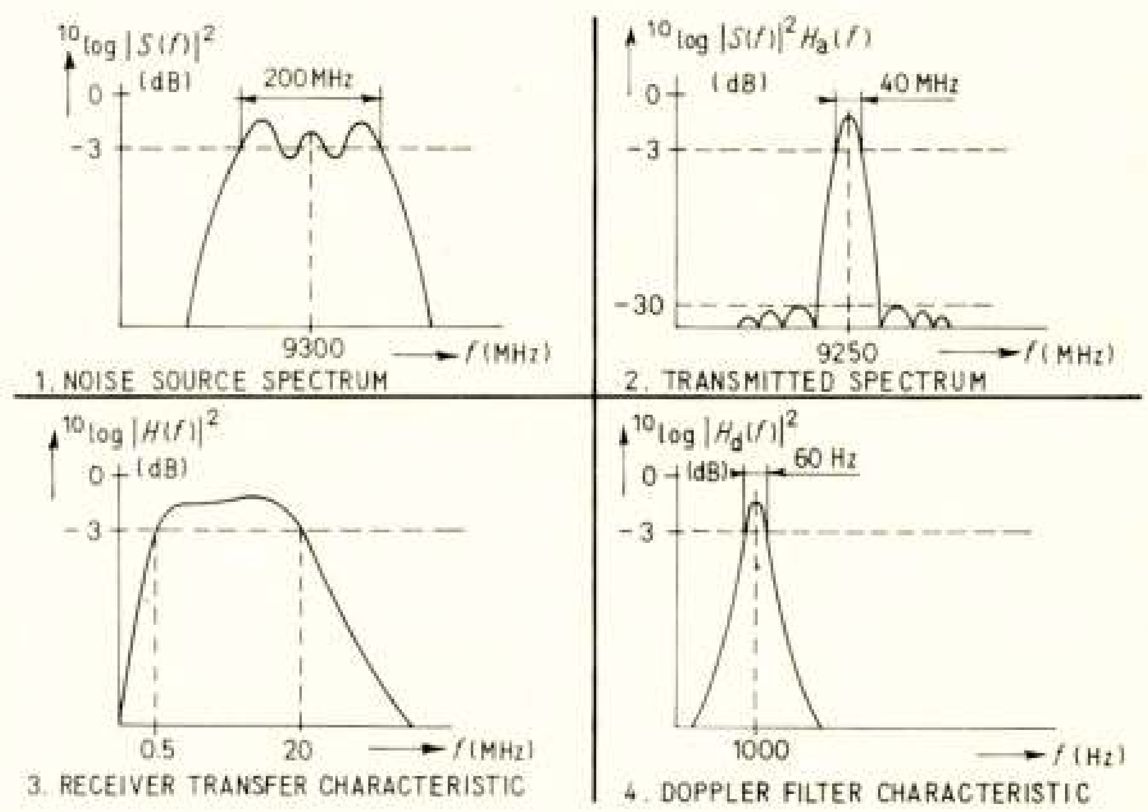


Fig. 6b. Spectra at some points in the RUDAR-system.

In Fig. 6a the block diagram of the realized system is given; Fig. 6b shows the spectra at some points of the system.

3.2. *Transmitter*

The transmitter consists of a noise source and of two travelling-wave tube amplifiers. As a noise source a fixed-frequency magnetron type JP 9-7A was used. It is possible to bring a magnetron into a condition of high noise output without stable or unstable oscillations. The best results were obtained by shunting the magnetron magnet. This shunt has a great influence on the spectrum form, while both the anode voltage and heater current will effect the output power. With a noise figure of 60 dB, a bandwidth of 200 MHz, and an amplifier gain of about 57 dB, the available output power was 350 MW.

3.3. *Antenna-system*

The antenna-system consists of two identical end-fed slotted waveguide aerials, with a length of 5.5 m. They are mounted with a special frame on a gearbox with servo-drive (Fig. 7). Each antenna has a beamwidth of 0.4° between the −3 dB points, a sidelobe level of −28 dB, and a gain of 35 dB. The squintfactor of this type of antenna is 8.83 × 10^{-3} °/MHz. With a uniform noise spectrum, the transmitted spectrum in a direction θ will be:

$$B_\theta = \frac{0.4}{8.83 \times 10^{-3}} = 45 \text{ MHz}$$

After reception with an identical antenna, the bandwidth is reduced to 22 MHz. The cross-coupling between antennas was about −70 dB, mainly due to the two-channel rotating joint. It could be improved to approximate −110 dB.

3.4. *Delay line*

To meet the specification for the delay line such as: a broad bandwidth of 200 MHz and a delay of at least 20 µs, a microwave delay line was used. This consists of a non-dispersive transmitting and receiving antenna system, a propagation path reasonably free of secondary obstructions, a reference target and a travelling-wave tube amplifier. In this delay line spurious responses were maximally 18 dB below the wanted signal. For this reason there was some inaccuracy in the measurements of correlation functions. A *variable delay line* was used in the video amplifiers, with a maximum delay of about 0.5 µs, adjustable in steps of 6.6 ns (= 1 m).

3.5. *Correlator performance*

The transfer function of the receivers is given in Fig. 8. With a uniform spectrum on the input of the mixers, the measured envelope of the cross-correlation function is as given in Fig. 9. The lack of symmetry indicates that the phase-transfer functions of the two amplifiers are not identical. Computer calculations give the phase difference function arg $H(f)$ of Fig. 10.

Time lacked to correct this difference. The sensitivity of the correlator receiver is dependent on the two input signal levels. In Fig. 11 this dependence is given for an output signal-to-noise ratio of 10. From this Figure it can be seen that there is an optimum level for the reference channel of about −50 dBm. This can be explained by the fact, that for small reference signals the conversion loss increases, while for greater reference signals the self-noise increases.

The output signal-to-noise ratio is dependent on the system function. If the power of the output signal- and noise-components are measured behind the low-frequency bandpass filter, the $(S/N)_{out}$ is [9]:

$$\left(\frac{S}{N}\right)_{out} = \frac{2B}{B_1} \frac{\frac{1}{2}\left(\frac{S}{N}\right)_1 \cdot \left(\frac{S}{N}\right)_2}{\left(\frac{S}{N}\right)_1 \cdot \left(\frac{S}{N}\right)_2 + \left[1+\left(\frac{S}{N}\right)_1\right] \cdot \left[1+\left(\frac{S}{N}\right)_2\right]}$$

where:

B = the effective bandwidth of the video receiver; (= 15.7 MHz);

B_1 = the effective bandwidth of the integration bandpass filter; (= 60 Hz);

$(S/N)_1$ = correlator input signal-to-noise ratio in signalling channel;

$(S/N)_2$ = correlator input signal-to-noise ratio in reference channel.

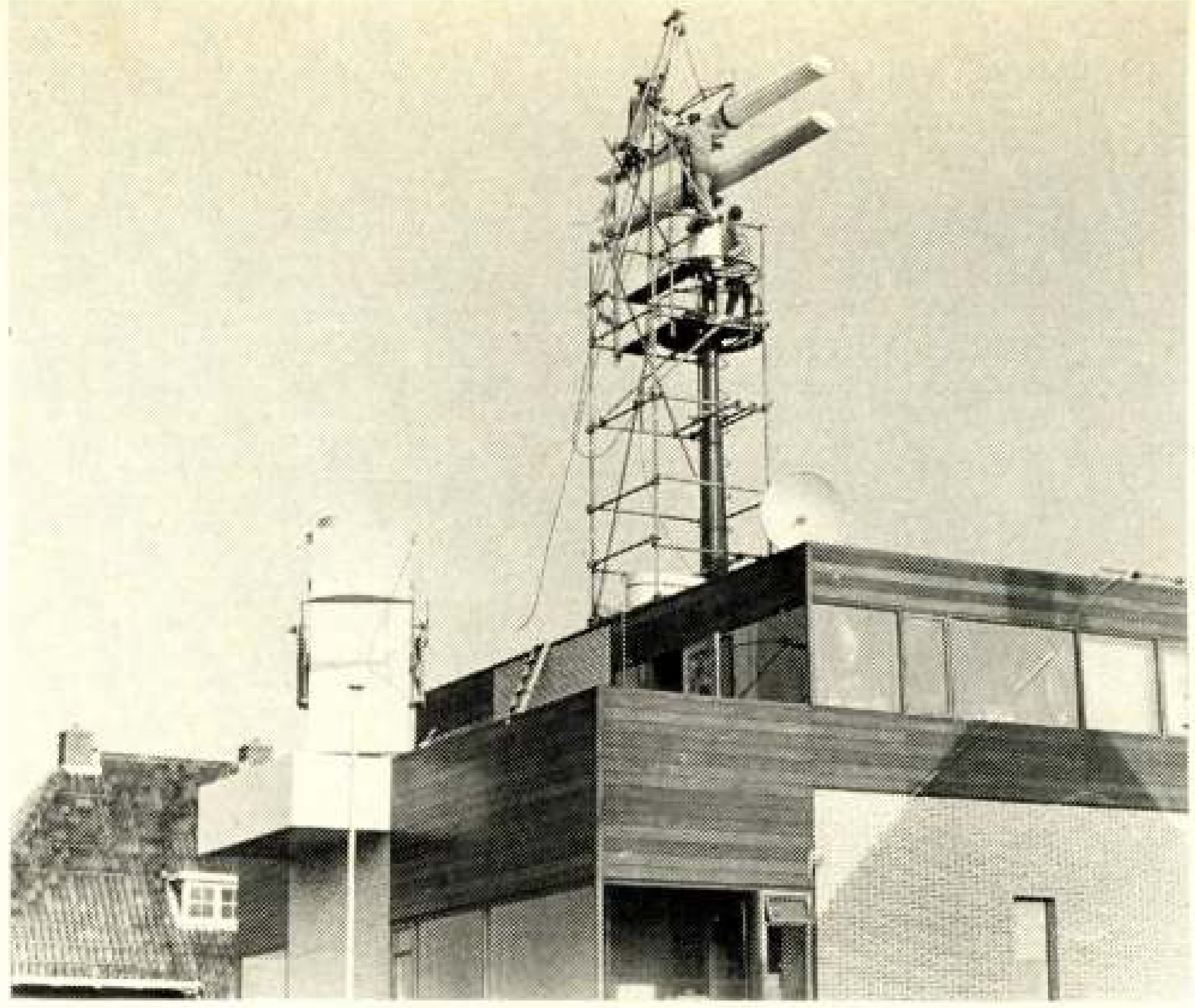


Fig. 7. The RUDAR antenna system.

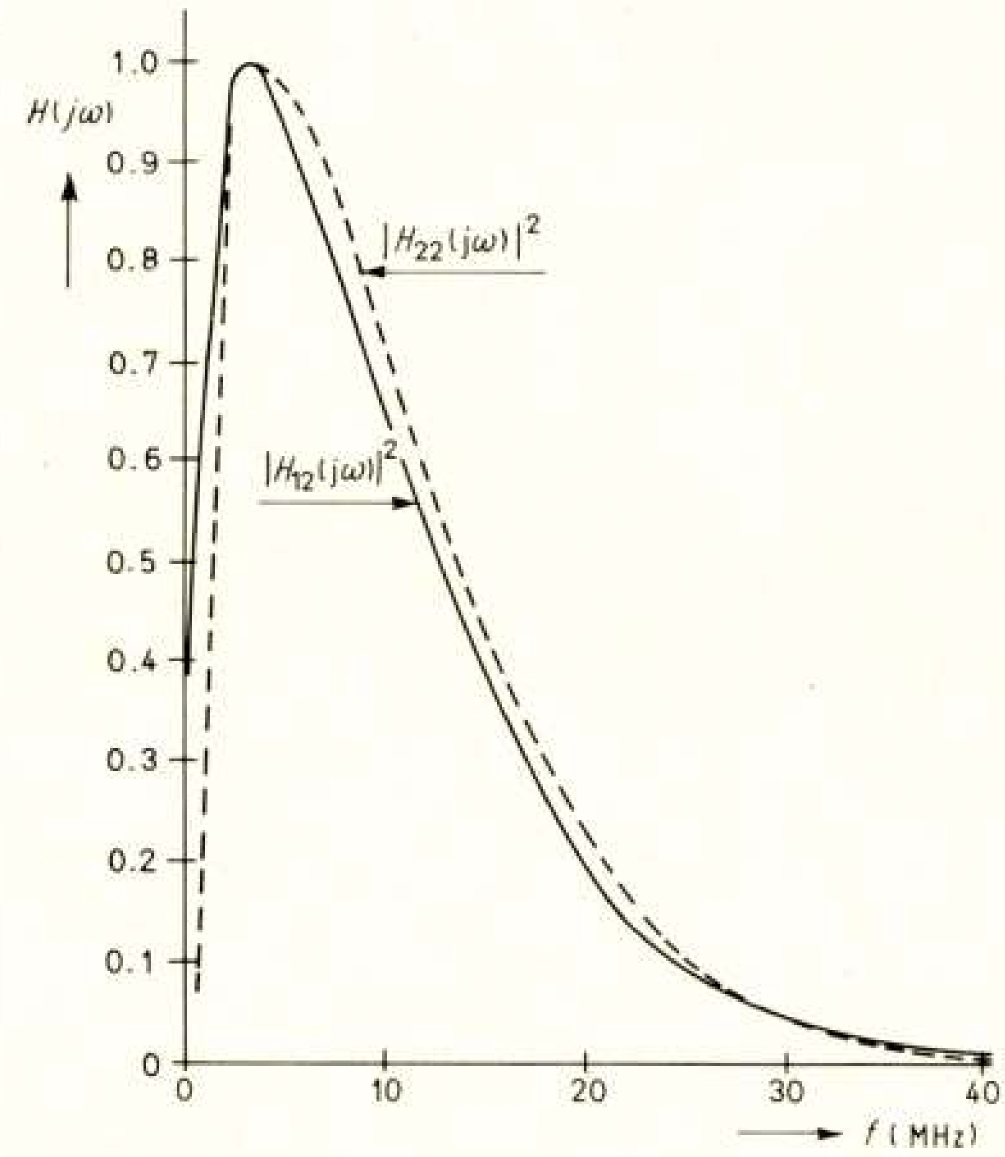


Fig. 8. Transfer function of correlator receivers.

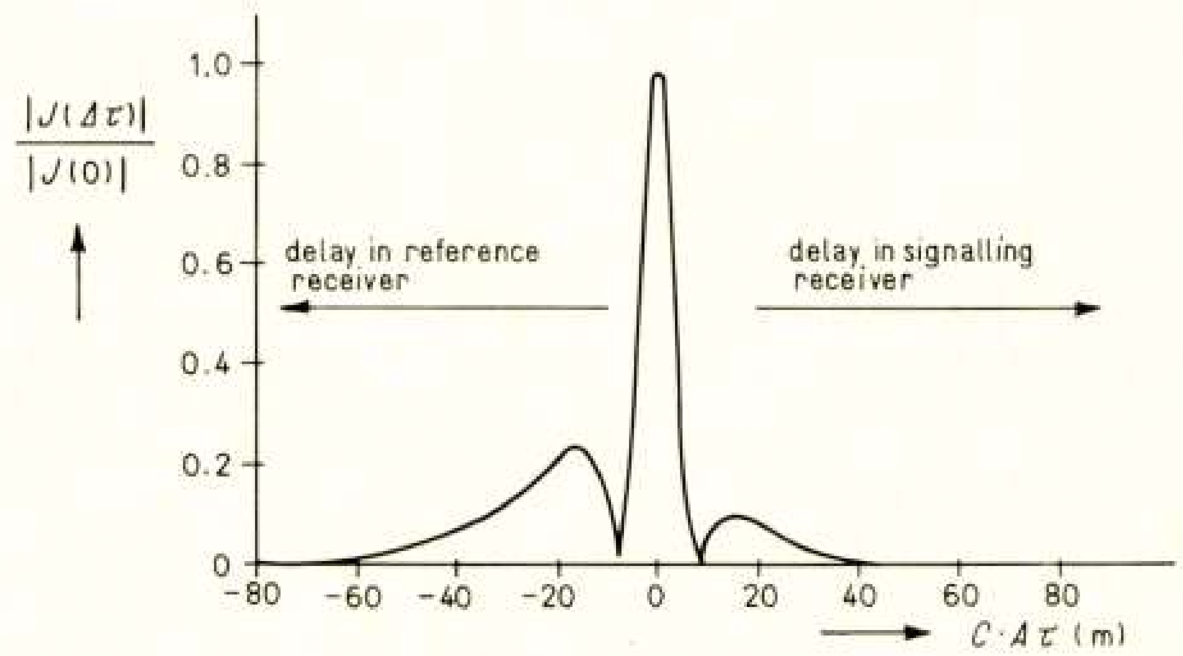


Fig. 9. Measured normalized envelope of the cross-correlation function of the RUDAR-receiver.

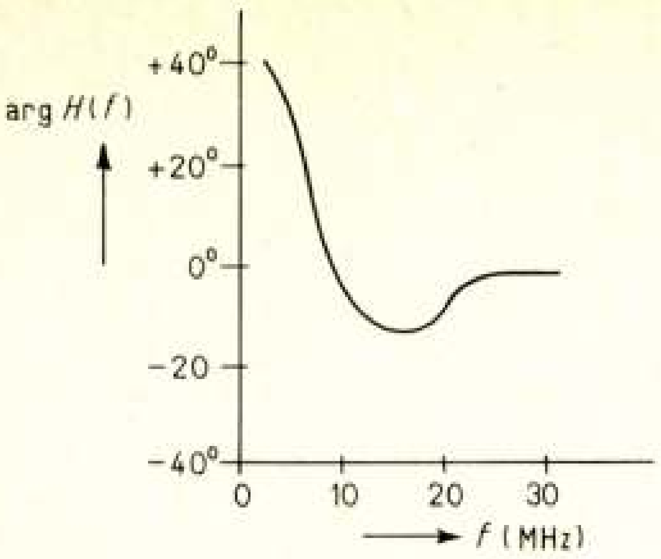


Fig. 10. Calculated phase-difference function of the correlator receiver.

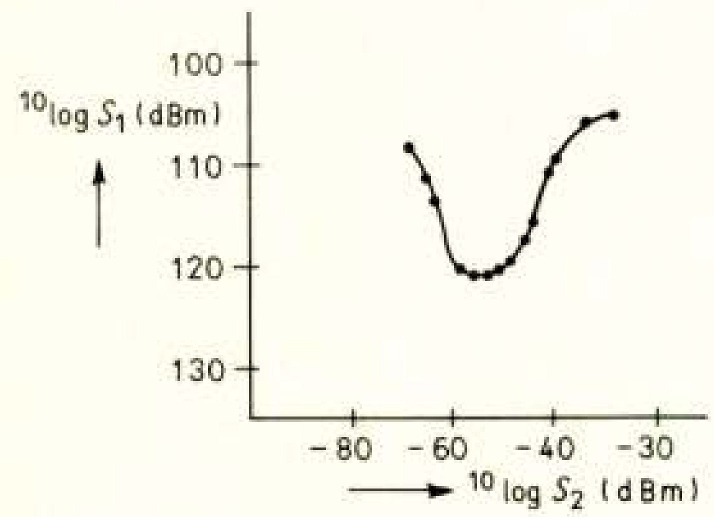


Fig. 11. Input signal level S_1 as a function of the reference signal level S_2 for (S/N) out = 10.

The input noise is partly of thermal origin and partly due to the cross-coupling effect:

$$N_{in} = N_t + \alpha \overline{P}_z$$

where:
N_t = input thermal noise power
α = the cross-coupling factor
P_z = average transmitted signal power.

In view of this the following signal-to-noise values were available:

$$10 \log \left(\frac{S}{N}\right)_1 = -35 \text{ dB}$$

$$10 \log \left(\frac{S}{N}\right)_2 = -10 \text{ dB}$$

The output signal-to-noise ratio in this case is:

$$10 \log \left(\frac{S}{N}\right)_{out} = +12 \text{ dB}$$

In the correlator circuit itself we found a maximum disagreement between theory and practice of about −4 dB, due to the 1/*f*-noise from the diodes in the multiplier circuit. Therefore a minimum output signal-to-noise ratio of +8 dB is to be expected.

3.6. *System possibilities*

The realized system possibilities are:
a. target detection under very low signal-to-noise conditions;
b. the antenna-system is used as a space filter;
c. as a result of b., there is an option for azimuth measurement by antenna rotation or by local oscillator frequency tuning, or a combination of both;
d. for distance measurement there is a choice between either microwave, I.F., or video delay lines, or a combination of the same;
e. by proper selection of signal bandwidth the accuracy of distance and bearing measurement can be exchanged;
f. radial target velocity is obtained by measuring the doppler-shift of the microwave signal. A reference doppler-shift can be introduced to measure different target velocities with a fixed filter.

4. Results

4.1. *Target detection*

For this measurement we used a conveniently situated fixed target. Detection can be accomplished by scanning in distance as well as in azimuth. Fig. 12 gives the result for azimuth scanning and a fixed delay; Fig. 13 the same for distance scanning and fixed bearing. From these Figures it can be seen that a signal-to-noise ratio of at least +8 dB has been realized. It has been therefore proved possible to detect a target with a noise radar.

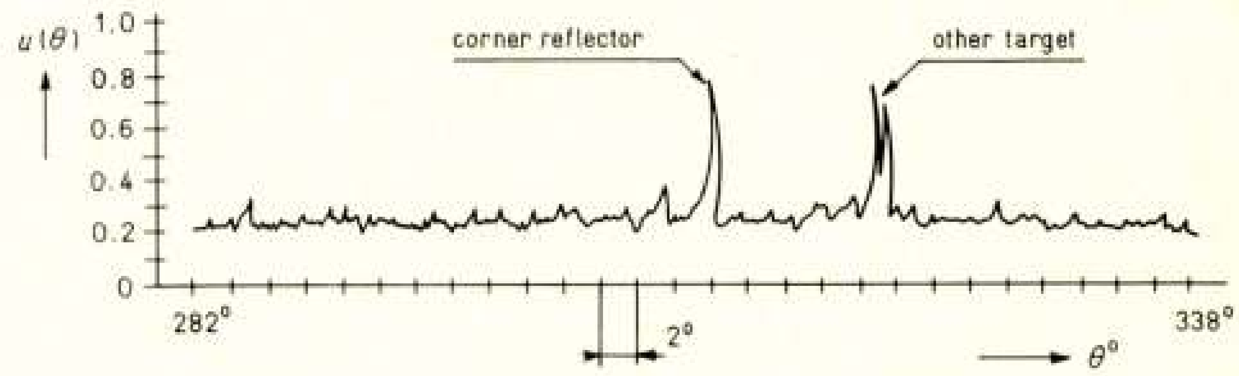


Fig. 12. Correlator output signal, for mechanical azimuth scanning over 50°.

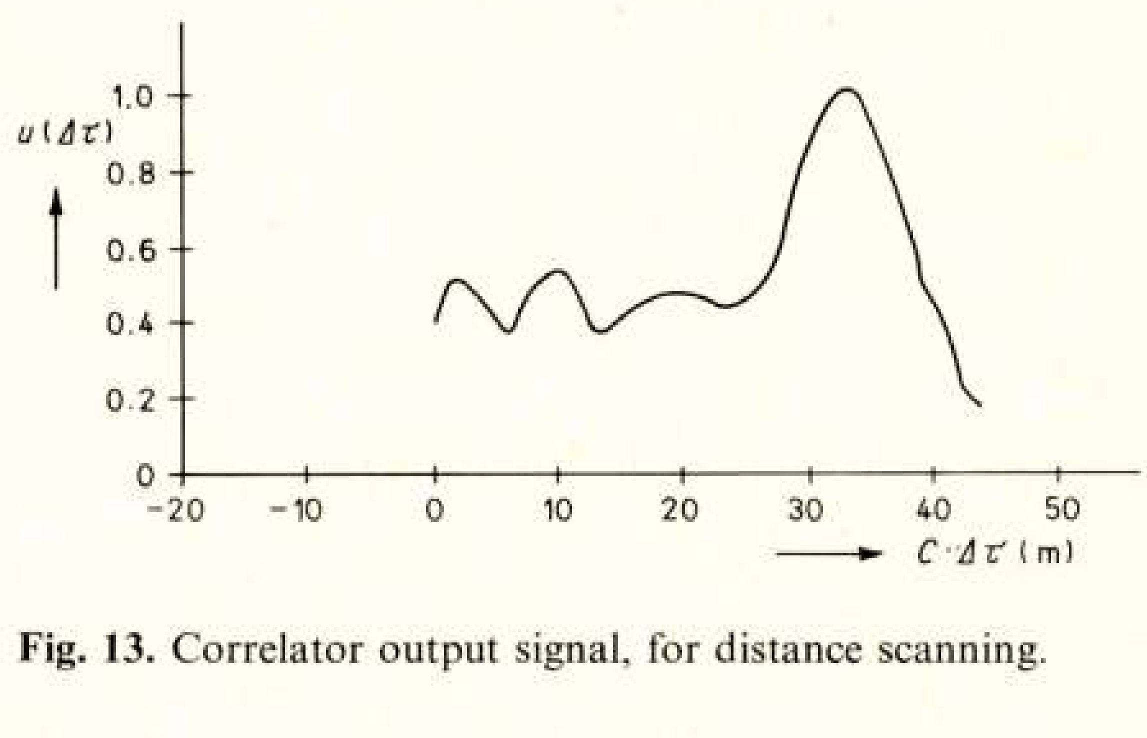


Fig. 13. Correlator output signal, for distance scanning.

4.2. *Frequency scanning*

For a linear array the relation between the direction of the mean beam (with respect to the normal) and the frequency (or wavelength λ) of a C.W.-signal is given by:

$$\sin \theta = \frac{\lambda}{\lambda_g} - \frac{\lambda}{\lambda_{g_0}} \quad \text{(Fig. 3).}$$

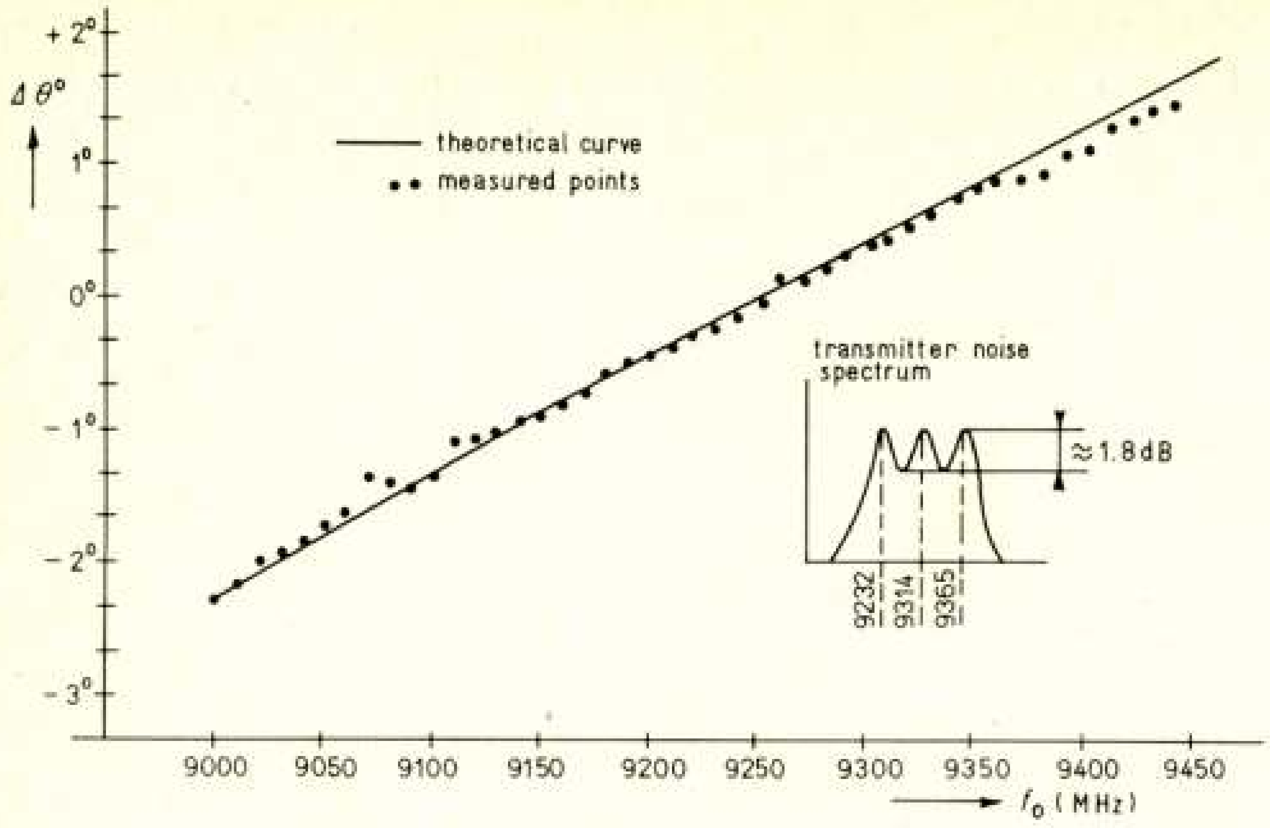


Fig. 14. Antenna-squint measurement with RUDAR (narrow video bandwidth).

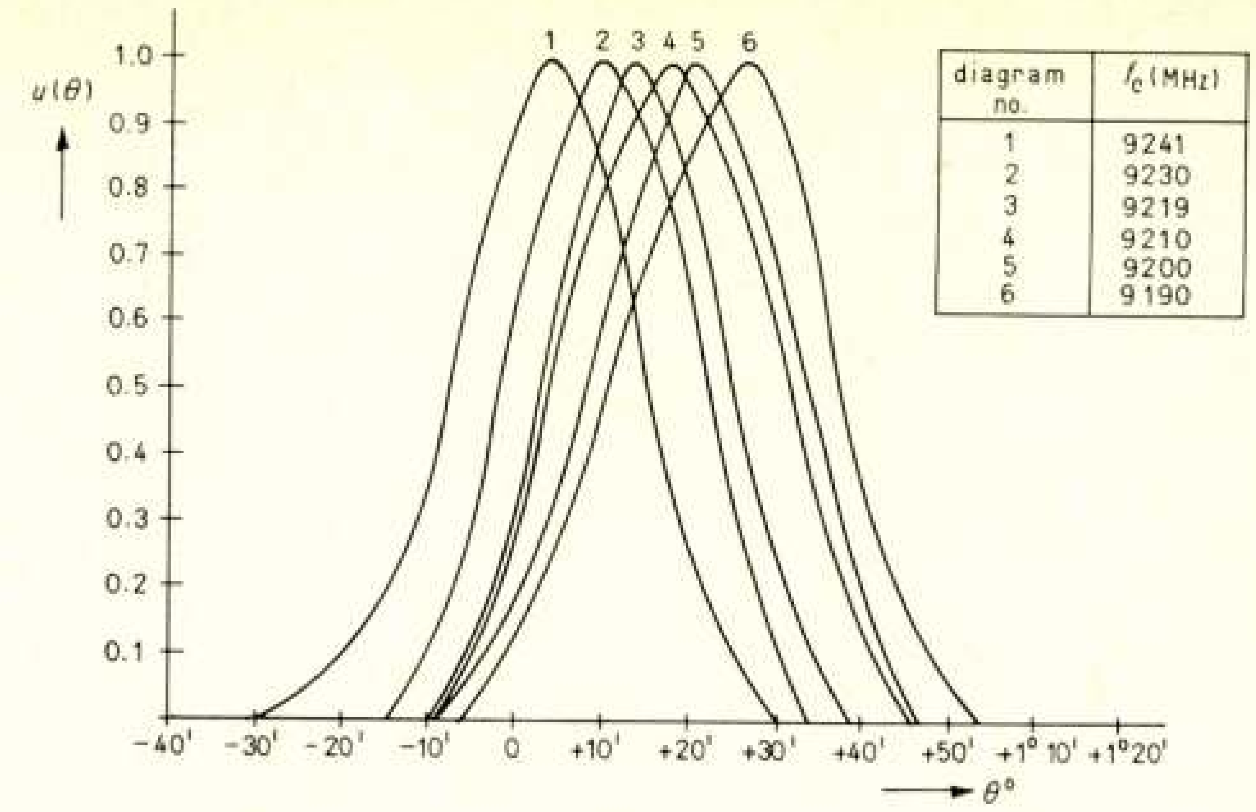


Fig. 15. Antenna system as space-filter (narrow video bandwidth).

An approximation for small angles is:

$\theta = K \Delta f$

with:

$\Delta f = f - f_{00}$

f_{00} = frequency for beam direction $\theta = 0$

K = squint factor: in this case: 8.83×10^{-3} °/MHz.

In Fig. 14 the results of the measurements are given where in stead of a C.W.-signal, a noise signal with a bandwidth of 14 MHz is used. The measured points of the mean beam direction are given along with the theoretical curve. The agreement is quite good.

The measured diagrams of the antenna system as a space filter are shown in Fig. 15. The signal bandwidth affects the accuracy of the bearing measurements. As long as the bandwidth of the receiver filter is smaller than the equivalent bandwidth of the antenna system, there is little loss in directivity. In the other cases a loss must be expected as can be seen in Fig. 16.

It will be obvious from the foregoing that there is a possibility to exchange accuracy in distance and direction. More details will be given in Appendix 7.2.

To check the correspondence of frequency- and mechanical azimuth scan we did two measurements:

a. with the antenna aimed at the target, the local-oscillator was swept over a broad frequency band and the correlator output was measured;
b. with the local-oscillator at a fixed frequency the antenna was rotated.

Fig. 17 shows the results obtained.

4.3. *Doppler measurements*

To get an insight into the behaviour of the system on moving targets we used a reference target (Fig. 18), and arranged for an artificial 'doppler shift' of ± 230 Hz. Instead of using a set of separate integration bandpass filters at the output of the correlator multiplier, the whole receiving system can be matched to the doppler shift by tuning the audio oscillator of the S.S.B. modulator to $(f_1 \pm 230)$ Hz.

In Fig. 19 the results are compared with a theory given by A. W. Rihaczek [14]. For targets with a constant range-rate the signal-to-clutter ratio can be expressed as the 'time-bandwidth'

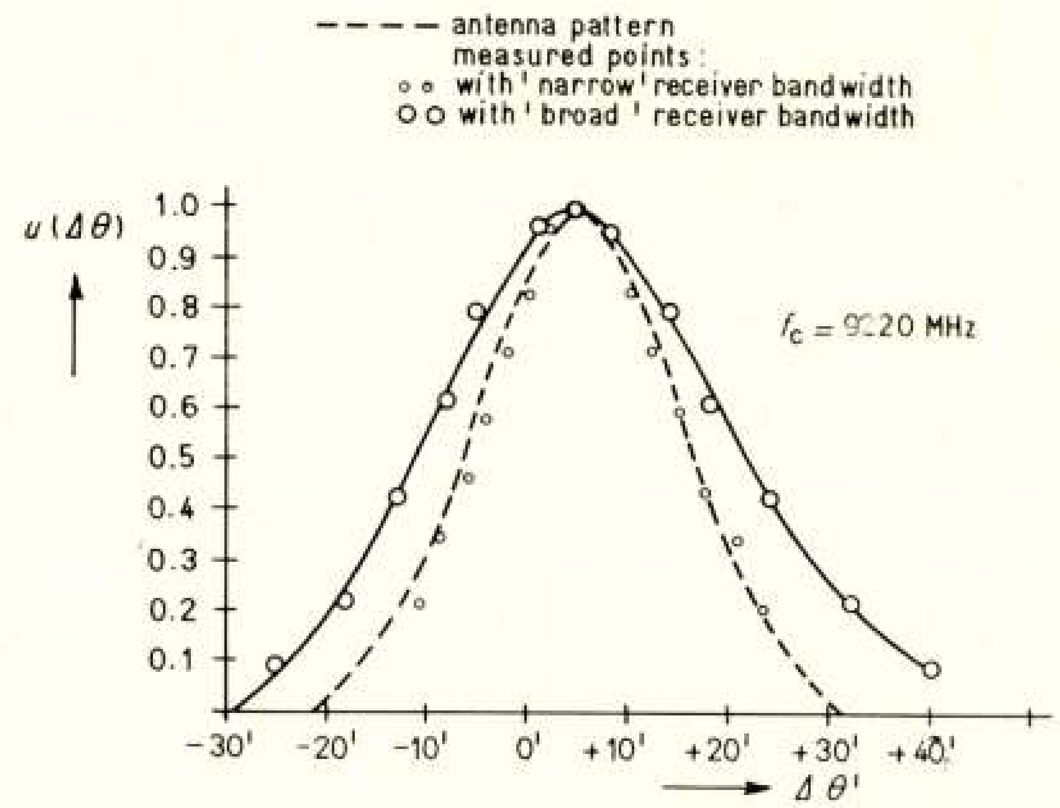


Fig. 16. Influence of receiver bandwidth on measured antenna main beam.

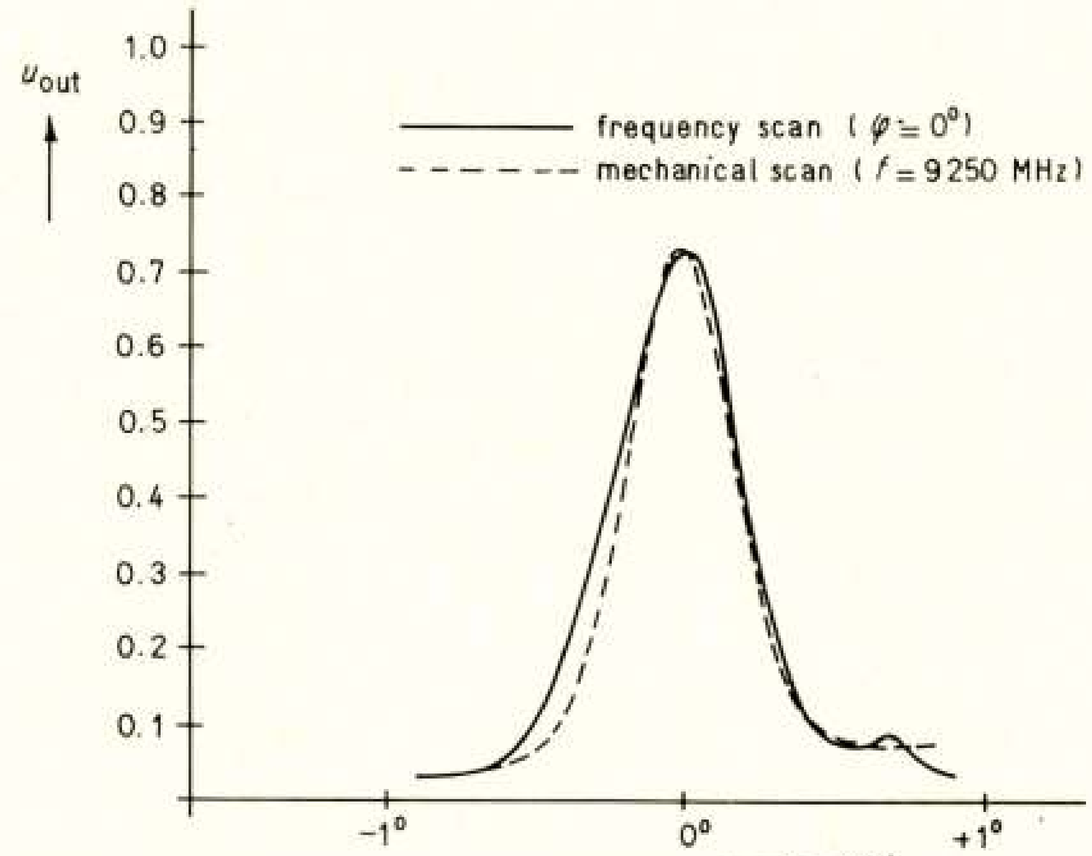


Fig. 17. Comparison of mechanical and frequency azimuth scanning.

product $(B_0 \cdot t_0)$, multiplied by the ratio of the 'target cross-section'-to-'total clutter cross-section'

$$\left(\frac{\sigma_r}{\sigma_{tot.}}\right).$$



Fig. 18. Corner-reflector as reference target on lorry.

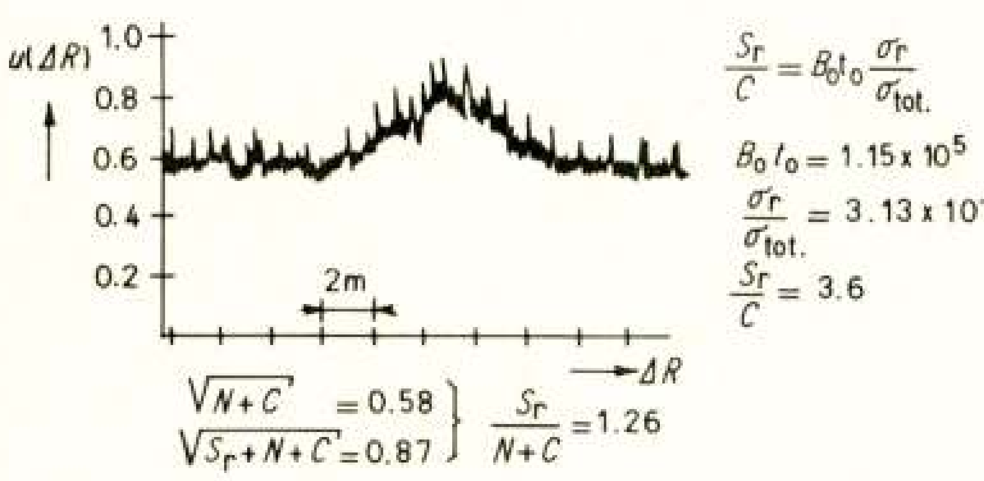


Fig. 19. Doppler measurement.

The values in our case are given in Fig. 19. The signal strength was about 44 dB below the clutter level. The output signal-to-clutter ratio had an expected value of 3.5. Actually a signal-to-(noise plus clutter) ratio of 1.26 was measured. The difference proved to be due to the $1/f$-noise contribution of the correlator.

With the method used it is possible to detect and measure the speed of moving targets against a background of fixed objects with a high clutter level.

5. Discussion of the results

On the base of these results it now becomes possible to check, in how far the objects of the experiment have been met.

5.1. *Test of the principle of noise radar*

5.1.1. It is indeed possible to detect a target in very poor S/N-conditions; even with non-optimum hardware with a $(S/N)_{in} = -35$ dB the $(S/N)_{out} \approx +12$ dB.

5.1.2. A dispersive linear array can be used as a space filter, even for a broadband noise signal. The measured relation between direction and frequency is in good agreement with the theoretical curve, provided the bandwidth of the transmitted spectrum is much greater than the receiver bandwidth. Mechanical and electrical scanning gave almost the same results. However, the electrical scanning method is very sensitive to interference, originating from spurious signals in the delay path.

5.1.3. Targets in the same space-cell but with different speeds can be resolved by measuring the doppler shift. The crosstalk between the different doppler channels is given by the filter characteristics.

5.1.4. In Appendix 7.2. a relation is given for the optimum bandwidth of the bearing filter. There will be little loss in bearing accuracy as long as the equivalent bandwidth of the video-filter is smaller than or equal to the antenna 'bandwidth': $B \leq \theta_{-3\,dB}/2K\sqrt{2}$. This agrees quite well with the measurements. The antenna pattern broadens as soon as the bandwidth of the bearing filter is greater than the bandwidth of the received signals. This results in fewer independent directions.

5.1.5. Bearing in mind that we would like to extrapolate the present results on one space-cell with one doppler-slot (one facet) to a system with $n \times m \times l$ facets, we can remark that:

- it is possible to get an insight in the behaviour of a complete system by comparing the different measurements for one facet;
- a specification can be given of filter- and amplifier-bandwidth, of amplification factors, of minimum noise factors, of maximum allowable spurious signals in delay lines, etc.;
- however, the dynamic behaviour of such a system of $n \times m$ cells cannot be predicted from these experiments;
- for the design of a more complex system the know-how of one facet is in fact essential; but multiplying the hardware of one facet to that of $n \times m \times l$ facets will not necessarily provide an optimum system.

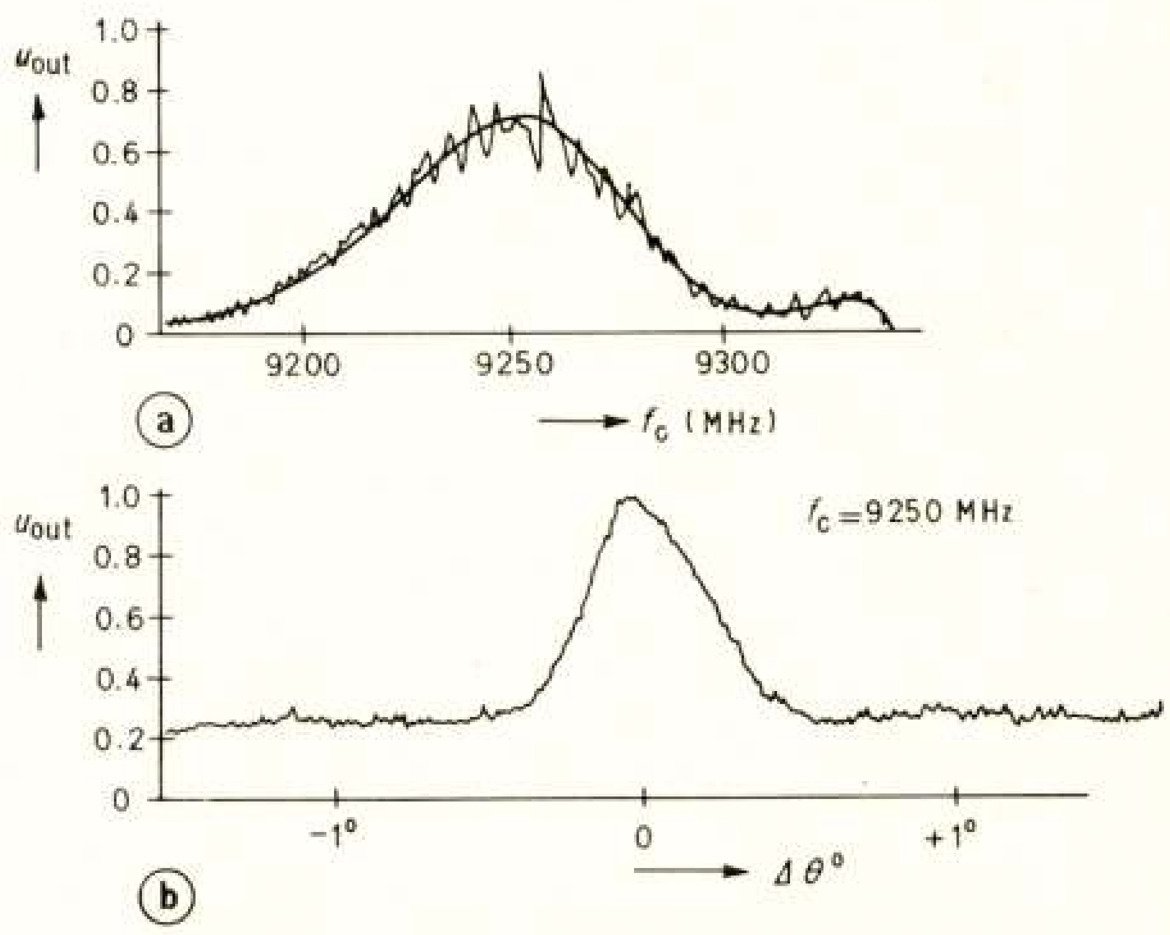


Fig. 20. Influence of spurious signals in delay line on frequency scanning: a. frequency scanning; b. mechanical scanning.

5.2. *The system's drawbacks*

The crosscoupling between transmitter- and receiver-antenna was about −70 dB. Because the transmitted power was not so high, the self-noise was below the $1/f$-noise of the correlator. This was also true for the nearby targets. However, the spurious signals in the delay line on the one hand, and the crosscoupling together with reflections from nearby targets on the other hand, gave correlated output signals. Especially with frequency scanning this effect was rather severe. In Fig. 20 the correlator output signal is given for frequency- resp. mechanical scanning. The interference effect of the target signal with the spurious signal is obvious from Fig. 20a. The correlator output signal in this case is [11]:

$$S_0(\Delta\tau_1, \Delta\tau_2, f_\Delta) = \tfrac{1}{2}[|J_1(f_\Delta)|^2 + |J_2(\Delta\tau_2, f_\Delta)|^2 + 2|J_1(f_\Delta)| \cdot$$
$$\cdot\, |J_2(\Delta\tau_2, f_\Delta)| \cos x\,(2f_c + f_\Delta) \cdot (\Delta\tau_2 - \Delta\tau_1)]$$

with:

$|J_1(f_\Delta)|^2$ = envelope of correlation function for the target

$|J_2(\Delta\tau_2, f_\Delta)|^2$ = envelope of correlation function for the spurious signal

$\Delta\tau_1$ = delay difference for target signal
$\Delta\tau_2$ = delay difference for spurious signal
f_Δ = $f_0 - f_c$
f_c = local oscillator frequency
f_0 = center frequency of antenna

A 2π phase variation in the interference term is obtained for a local oscillator variation of:

$$f_{c_1} - f_{c_2} = \frac{2}{\Delta\tau_2 - \Delta\tau_1}$$

In our case there was a delay difference of $\Delta\tau_2 - \Delta\tau_1 = 0.33$ µs that would give a 2π phase variation for every 6 MHz of local oscillator variation. This agrees quite well with the measured results. For a 1% output fluctuation and a value of $(S/N)_{in} = 10^{-3}$, the spurious signal in the delay line must at least be 50 dB below the wanted signal.

5.3. *The measurement accuracy*

The accuracy of the measurement depends on the output signal-to-noise ratio and on the presence of interfering objects. In view of 5.2., both were not too good, unfortunately. Differences of 1 m in the distance to one target could easily be measured. The resolution between two targets was about 30 m. The measured antenna squint characteristic agrees well with the theoretical curve. Deviations were caused by the non-uniform transmitter spectrum.

6. Conclusion

From the discussion of the measurements it has been shown that a noise radar can be realized. Also it has been proved that the spectrum of a noise signal can be spread out in space with a dispersive array, and that position (distance, bearing) and velocity of a target can be measured.

The difficulties that appear in the realization of such a system are many. This experiment has been very useful to recognize these difficulties, to learn their importance, and if possible to deal with them.

The results obtained with a dispersive linear array have a more general importance in that they can easily be extrapolated to the case of a two-dimensional dispersive array (Fig. 21).

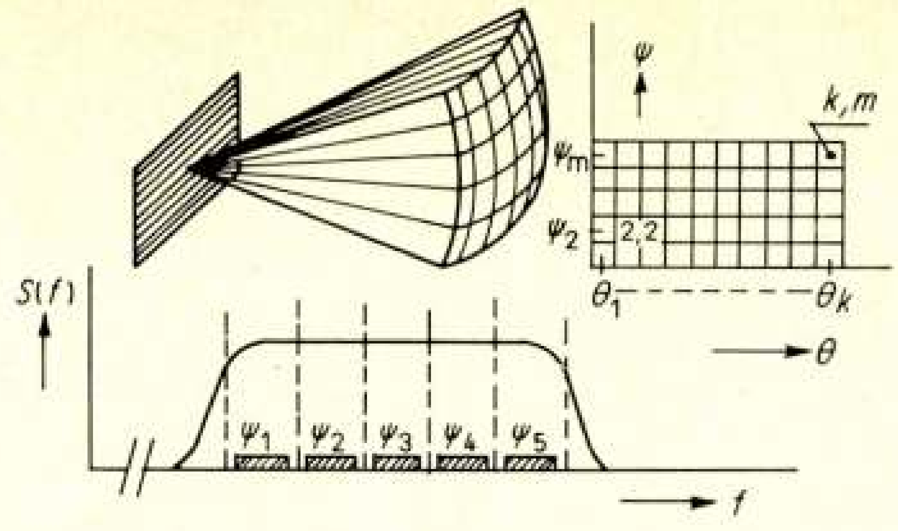


Fig. 21. Two-dimensional array.

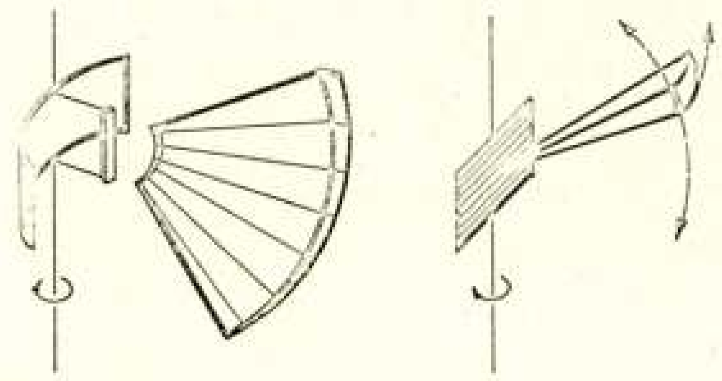


Fig. 22. Combination of mechanical and frequency scanning.

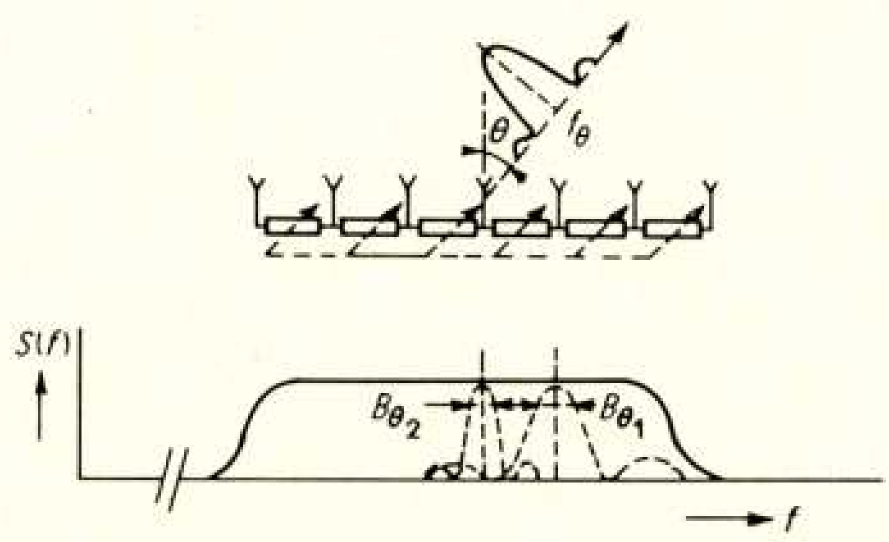


Fig. 23. Dispersive linear array with variable squint.

In such a manner the broadband noise signal can be dispersed in two independent co-ordinates, viz. azimuth (θ) and elevation (ψ). Every direction in space, defined by θ and ψ, is uniquely determined by a specific center frequency of a spectrum, characterized by the squint factors K_a and K_e. The form of the spectrum will depend on the antenna pattern as before. So it should be possible to obtain in one measurement target position in three dimensions (τ, θ, ψ).

Attractive possibilities arise when combining mechanical and frequency-scanning. For instance θ by mechanical scan and ψ by frequency scan (Fig. 22).

Alternatively when scanning in one co-ordinate the combination in mechanical- and frequency-scan offers the possibility to improve the dwell-time on a target.

So far the squint factor K was supposed to be a constant. A

further possibility is making this squint factor K a system-variable (Fig. 23), for example by means of varying the line lengths between the radiating elements. For a certain direction θ, the spectrum for two values of K is shown. As K increases, the spectrum bandwidth decreases, and so does the center frequency.

Every type of signal has its own limitations. As is known from literature, the usefulness of a random noise signal, just as every continuous signal, is limited by the target environment. Methods to overcome this limitation have been studied [4, 15]. The system's hardware could be another limitation.

The decision whether to use a random noise signal for a particular application can only be arrived at by careful consideration of its weighted advantages and disadvantages.

It was the aim of this paper to demonstrate the feasibility of the use of noise as a radar signal, and to provide sufficient insight for visualized applications.

7. Appendix

7.1. *Microwave envelope-correlators*

In the following a discussion will be given of three methods to construct an envelope-correlator. These methods are shown in Fig. 4a ... c. We shall use the complex-signal notation [13, 14].

7.1.1. *Single-sideband modulator and bandpass correlator*

In Fig. 4a the block diagram is given. In this relatively simple structure the filters F_1 and F_2 are supposed to be microwave filters. Filter F_1 selects a frequency band from the reference signal. The combination of the dispersive antenna and filter F_2 provides the bearing of the detected signals. It will be shown that this circuit yields the envelope of the correlation function. After the filters F_1 and F_2 we have the signals:

$$S_1(t+\tau_1) = \mathrm{Re}\left[\mu_1(t+\tau_1)\, e^{j2\pi f_0(t+\tau_1)}\right]$$

$$S_2(t+\tau_2) = \mathrm{Re}\left[\mu_2(t+\tau_2)\, e^{j2\pi f_0(t+\tau_2)}\right]$$

$\mu_1(t)$ and $\mu_2(t)$ are low-frequency functions with respect to the carrier f_0. The two signals originated from the same source and have different delay paths τ_1 and τ_2.

$x_A(t)$ is the output signal of the single-sideband mixer:

$$x_A(t) = \left[a(t)\cdot S_1(t+\tau_1)\right]_{f_0+f_m}$$

with:

$$a(t) = A\,\mathrm{Re}\left[e^{j2\pi f_m}\right]$$

$$x_A(t) = \frac{A}{2}\mathrm{Re}\left[\mu_1(t+\tau_1)\, e^{j2\pi(f_0+f_m)(t+\tau_1)}\right] +$$

$$+\gamma\frac{A}{2}\mathrm{Re}\left[\mu_1(t+\tau_2)\, e^{j2\pi(f_0-f_m)(t+\tau_1)}\right]$$

where $\gamma < t$, and gives the suppression of the unwanted sideband. The multiplier circuit gives:

$$y(t) = \left[S_2(t)\cdot x_A(t)\right] =$$

$$= \frac{A}{4}\mathrm{Re}\left[\mu_1(t+\tau_1)\,\mu_2(t+\tau_2)\, e^{j2\pi f_m(t+\tau_1)}\, e^{j2\pi f_m(\tau_1-\tau_2)}\right] +$$

$$+\gamma\frac{A}{4}\mathrm{Re}\left[\mu_1^*(t+\tau_1)\,\mu_2(t+\tau_2)\, e^{j2\pi f_m(t+\tau_1)}\, e^{-j2\pi f_m(\tau_1-\tau_2)}\right]$$

The integration bandpassfilter has an impulse response

$$h(t) = \mathrm{Re}\left[h_0(t)\, e^{j2\pi f_m t}\right]$$

with $h_0(t)$ a real function.
After this filter we get:

$$g(t) = \mathrm{Re}\,\tfrac{1}{2}\left[\int_{-\infty}^{+\infty} h_0(\xi)\left\{x_A(t-\xi) - S_2(t-\xi)\right\}\cdot e^{j2\pi f_m \xi}\, d\xi\right]$$

The following relations are used:

$$\mu_1(t+\tau_1) = \int_{-\infty}^{+\infty} M_1(f)\, e^{j2\pi f(t+\tau_1)}\, df$$

$$\mu_2(t+\tau_2) = \int_{-\infty}^{+\infty} M_2(f')\, e^{j2\pi f'(t+\tau_2)}\, df'$$

$$Z(f) = \int_{-\infty}^{+\infty} h_0(\xi)\, e^{-j2\pi f\xi}\, d\xi = 2H(f) \text{ if } f>0$$
$$= 0 \quad \text{if } f<0$$

For the 'signal' part of $g(t)$ we could write, with:

$f = f'$; $Z(0) = 2$, and $\tau_1 - \tau_2 = \tau$:

$$g_{\mathrm{sign.}}(t) = \mathrm{Re}\left[\frac{A}{4}\int_{-\infty}^{+\infty} M_1(f)\, M_2^*(f)\, e^{j2\pi f\tau}\, df\cdot e^{j2\pi\{f_m(t+\tau_1)+f_0\tau\}}\right.$$
$$\left. +\gamma\frac{A}{4}\int_{-\infty}^{+\infty} M_1^*(f)\, M_2(f)\, e^{j2\pi f\tau}\, df\cdot e^{j2\pi\{f_m(t+\tau_1)+f_0\tau\}}\right]$$

The signals $S_1(t)$ and $S_2(t)$ originate from the same source but have traversed different paths with frequency amplitude characteristics $H_1(f)$ and $H_2(f)$:

$M_1(f) = W_s(f)\cdot H_1(f)$
$M_2(f) = W_s(f)\cdot H_2(f)$

where:

$W_s(f) = \psi_s(f+f_0)$, is the spectrum of the complex envelope of the source signal:

$$\Psi_s(f) = 2\,S(f) \text{ for } f>0$$
$$= 0 \quad \text{for } f<0$$

Substitution of these functions will give for the envelope of $g_{\mathrm{sign.}}(t)$:

$$|g_{\mathrm{sign.}}(t)| = A\sqrt{1+\gamma^2+2\gamma\cos 2\alpha}\cdot\sqrt{\mathrm{Re}^2 J(t) + \mathrm{Im}^2 J(\tau)}$$

With a detector after the bandpass filter the envelope of the correlation function can be measured. To scan in azimuth the filters F_1 and F_2 must be varied synchronously.

The S.S.B.-modulator must be suitable for a bandwidth of 200 MHz.

The multiplier circuit is a balanced mixer with microwave mixer-diodes.

For a frequency azimuth-scan this circuit also must have a bandwidth of 200 MHz.

An acceptable conversion loss can be obtained with 1 mW of reference signal power on the output of the S.S.B.-modulator. The multiplier circuit must be well balanced, especially so to eliminate the mix-products of the spectrum of the strong refer-

ence signal. An unbalance better than 25 dB below the input signal is not to be expected for signals with bandwidths of 20 MHz lying within a band of 200 MHz.

Therefore it is recommended to choose the center frequency of the narrow bandpass filter outside this spectrum.

A suppression of the unwanted sideband in the S.S.B.-modulator, better than 20 dB is not to be expected, so the measured envelope of the correlation function has a ripple of about $\pm$ 10%.

A disadvantage of this S.S.B.-modulator is the small permissible signal level, the internal noise contribution, and the conversion loss of 8 to 10 dB.

From the results of experiments with a set-up according to this method, we found that for an output signal-to-noise ratio of 10 dB, an interference-free input signal level of about -70 dB (with a bandwidth of 20 MHz), is needed. This method is not suitable for a radar system because:
- the sensitivity is too low;
- the filters F_1 and F_2 must be tuned synchronously and with high precision.

7.1.2. *Combination of a normal correlator with a '90°'-correlator*

In Fig. 4b an example is given: a mixer circuit in front of the multiplier circuit shifts the spectra of the signals to a band where it is possible to use conventional amplifiers.

These amplifiers could also be used as selective directional filters. When choosing the intermediate frequency, care must be taken to eliminate the image frequency band.

Therefore pre-selection filters will be necessary. In principle, azimuth scanning is possible by tuning of the local-oscillator. It is possible to use an I.F.-delay line. A special case, approaching the third method to be mentioned in 7.1.3., arises when f_0 is in the middle of the spectrum of $s(t)$.

The filters F_1, F_2 and F_3, and the amplifiers become low-pass circuits with bandwidths that are about half the bandwidth of the incoming signals. It is now even possible to use video delay lines. Moreover the problem of the rejection of the image frequencies is thereby avoided.

It is very important to equalize the conversion loss in the multiplier circuit and the amplification in channels 2 and 3.

The construction of a circuit for squaring correlation functions with sufficient stability and dynamic range is not easy. The output signal is the square of the envelope of the correlation function. A derivation will be given below.

The input signals are again $S_1(t+\tau_1)$ and $S_2(t+\tau_2)$ (see 7.1.1.). These signals are mixed with:

$$a(t) = A\ \mathrm{Re}\left[e^{j2\pi f_c t}\right]$$

$$b(t) = A\ \mathrm{Im}\left[e^{j2\pi f_c t}\right]$$

The output signals of the mixers are filtered in the I.F.-amplifiers, whereupon the multiplications $x_A(t)\cdot x_B(t)$ and $x_A(t)\cdot x_c(t)$ are made.

The derivation is analogous to the method given in 7.1.1. With an integration time large with respect to the correlation time of the signals and $H_{22}(f) \equiv H_{32}(f)$, it is easy to show that the output signal becomes:

$$\mu_{out}(\tau) = \left(\frac{A^2}{4}\right)^2 \left[\mathrm{Re}^2\, J(\tau) + \mathrm{Im}^2\, J(\tau)\right]$$

with:

$$J(\tau) = \int_{-\infty}^{+\infty} M_1(f)\, M_2^*(f)\, H_{12}(f)\, H_{32}^*(f)\, e^{j2\pi f\tau}\, df$$

7.1.3. *Bandpass correlator with video amplifiers*

The correlator receiver element for the present radar system has been built according to this principle (Fig. 4 ... c). Again the input signals are $S_1(t+\tau_1)$ and $S_2(t+\tau_2)$.

The local oscillator signals are:

$$a(t) = A\ \mathrm{Re}\left[e^{j2\pi f_c t}\right]$$

and a signal that is shifted in frequency by an S.S.B.-modulator over f_1 Hz ($f_1 < 1$ MHz):

$$b(t) = B\ \mathrm{Re}\left[e^{j2\pi (f_c + f_1)t}\right]$$

The frequency-difference terms in the mixer output signals will be passed by the video filters.

After the video amplifiers, with frequency amplitude characteristics $H_{12}(f)$ and $H_{22}(f)$ we get the signals $x_A(t)$, resp. $x_B(t)$. The signal $\{x_A(t)\cdot x_B(t)\}$ is integrated in a bandpass filter tuned to f_1. The envelope of the signal term of the output signal is:

$$\left|g_{sign.}(t)\right| = \frac{AB}{2}\sqrt{\mathrm{Re}^2\, J(\tau) + \mathrm{Im}^2\, J(\tau)}$$

with:

$$J(\tau) = \int_{-\infty}^{+\infty} |S(f+f_c)|^2\, H_{11}(f)\, H_{12}(f)\, H_{21}^*(f)\, H_{22}^*(f)\, e^{j2\pi f\tau}\, df$$

In the video amplifiers it is possible to delay the signals by a video delay line. The bandwidth of this delay line may be half the bandwidth of the received signals. By choosing f_c somewhere inside the spectrum of the signals $w_1(t)$ and $w_2(t)$, $s_1(t)$ and $s_2(t)$ are selected and band-limited by the low-pass filters F_1 and F_2. The correlator input signals are selected rather with filters symmetric about f_c and with a pass band given by F_1 and F_2. Azimuth scanning is obtained by tuning of the local oscillator.

The frequency shift f_1 is essential for the determination of the envelope of the correlation function.

Without this frequency shift, the correlation function with fine structure would be measured as a D.C.-signal. Choosing $f_1 < 1$ MHz has various advantages:
- the filters F_1 and F_2 can be identical, when $f_1 \ll$ bandwidth of the filters;
- if F_1 and F_2 are not real low-pass filters, but have a cut-off frequency $> f_1$, signals with frequencies f_1 resulting from the S.S.B.-modulator, as a result of cross-talk, are suppressed;
- the $1/f$-noise from the microwave mixer-diodes is also suppressed;
- integration filters with a bandwidth of about 100 Hz are easily realized.

7.2. *Influence of receiver bandwidth on bearing resolution*

The amplitude transfer characteristics of a linear array in a direction θ is:

$$H_a(f', \theta) = \frac{\lambda_c}{a} \int_{-\frac{a}{2\lambda c}}^{+\frac{a}{2\lambda c}} A(x)\, e^{j2\pi x u(f', \theta)}\, dx$$

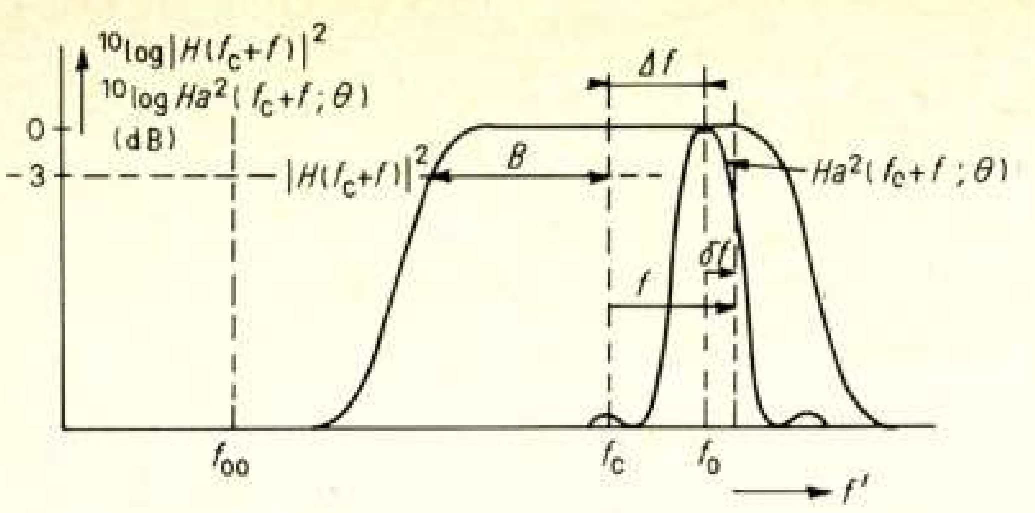


Fig. 24. Frequency relationship between antenna and receiver filter.

with:

a = length of the array

$A(x)$ = the illumination function

$$u(f',\theta) = v - \frac{f_{00}}{f'}\, v_{00} = \sin\theta$$

$$v = \frac{\lambda}{\lambda_g}$$

$$\theta = 0 \text{ for } f' = f_{00}$$

If the antenna is aimed at a target in a direction θ_0, and the receiver is tuned to a center frequency f_0 (Fig. 24), we have for $f' = f_0$: $u(f_0, \theta_0) = 0$, and $\sin\theta_0 = K(f_0 - f_{00})$;
for $f' = f_0 + \delta f = f_c + f$: $u(f_c + f) = \sin\theta_c - \sin\theta_0 + Kf$, with $\sin\theta_c - \sin\theta_0 = K(f_c - f_0)$.

$K = v_{00}/f_{00}$, and is approximately constant for small frequency deviations.

In case of a constant local oscillator frequency f_c and a rotating antenna, θ_c is constant and θ_0 is the variable azimuth angle with respect to the normal to the array.

For a constant delay difference τ, the output of the correlator will give an 'antenna pattern' with center θ_c.

This antenna pattern is measured as the envelope of the correlator output signal:

$$|J(\tau,\Delta\theta)| = \left|\int_{-\infty}^{+\infty} |S(f+f_c)|^2\, H_{at}(f)\, H_{ar}(f)\, H_{12}(f)\, H^*_{21}(f)\, H^*_{22}(f)\, e^{j2\pi f\tau}\, df\right|$$

with:

$|S(f+f_c)|^2$ = noise source power spectrum

$H_{at}(f)$ = amplitude transfer characteristic of transmitting antenna

$H_{ar}(f)$ = the same for the receiving antenna

$\Delta\theta = \theta_c - \theta_0$

For a symmetrical illumination function $A(x)$, $H_a(f)$ is a real function. If the transmitting- and receiving-antenna are identical:

$H_{at}(f) = H_{ar}(f) = H_a(f)$

$H_{12}(f)$ and $H_{22}(f)$ are the receiver filter amplitude transfer characteristics.

$H_{21}(f)$ is the amplitude transfer characteristics for some other filter.

The matching condition for maximum output signal and constant $\Delta\theta$, is:

$H_a^2(f) \cdot H_{12}(f) = H_{21}(f) \cdot H_{22}(f)$

The two receiver filters are made identical to ensure equal phase functions, while $H_{21}(f)$ could be used as a correction filter in case of an asymmetric $A(x)$. With these assumptions we get:

$H_{12}(f) = H_{22}(f) = H(f)$

$H_{21}(f) = 1$

With a broad uniform source spectrum, the normalized antenna bearing characteristic will be:

$$\frac{|J(0,\Delta\theta)|}{|J(0,0)|} = \frac{\left|\int_{-\infty}^{+\infty} |H(f)|^2 \{H_a(\Delta\theta + Kf)\}^2\, df\right|}{\left|\int_{-\infty}^{+\infty} |H(f)|^2 \{H_a(Kf)\}^2\, df\right|}$$

Insight in the influence of the receiver bandwidth on the bearing resolution can be obtained by using some approximations. For instance if the filter transfer function is a gaussian function and the standard deviation is defined as $\sigma_H = B/D$, then $D = 1{,}179$

if: B = the bandwidth between $f = 0$ and $f = f_{-3\,dB}$.

The same is done for the antenna, for which the standard deviation is:

$$\sigma_a = \frac{\theta - 3dB}{2D}$$

with:

$\theta_{-3\,dB}$ = the antenna beamwidth between the -3 dB points.

The normalized antenna characteristic becomes in this case:

$$\frac{|J(0,\Delta\theta)|}{|J(0,0)|} = \exp\left[-\frac{1}{2}\frac{(\Delta\theta)^2}{\frac{K^2}{D^2}\left\{B^2 + \left(\frac{\theta_{-3dB}}{2K\sqrt{2}}\right)^2\right\}}\right]$$

The 'beamwidth' of this pattern will be:

$$\theta'_{-3dB} = 2K\sqrt{B^2 + \left(\frac{\theta_{-3dB}}{2K\sqrt{2}}\right)^2}$$

A measure of the loss in the angular resolution could be defined as the ratio:

$$\eta = \frac{\theta_{-3dB}}{\theta'_{-3dB}} = \frac{1}{\sqrt{1 + \left(\frac{2BK\sqrt{2}}{\theta_{-3dB}}\right)^2}}$$

In the experiment we used two video bandwidths which where equivalent resp. to a 'broad' R.F.-bandwidth of about 30 MHz and a 'narrow' R.F.-bandwidth of about 14 MHz.

The antenna beamwidth was 0.4°.

For the two cases we obtain respectively:

with $2B$ = 30 MHz: $\eta = 0{,}73$

with $2B$ = 14 MHz: $\eta = 0{,}91$

From the measurements (Fig. 16) follows resp.: $\eta = 0{,}71$ and $\eta \approx 1$. This agrees quite well.

It can be shown that the receiver bandwidth B, which would give joint optimum resolution in distance as well as in angle is given bij the relation:

$$B = \frac{\theta_{-3dB}}{2K\sqrt{2}}$$

References

[1] Siebert, W. M.: A radar detection philosophy. I.R.E. Trans. I.T.-2, Sept. 1966, p. 204.

[2] Grant, M. P., e.a.: A class of Noise Radar Systems. Proc. I.E.E.E., July 1963, p. 1060.

[3] CARPENTIER, M.: Radars, Concepts Nouveaux. Dunod, Paris 1966.
[4] WOODWARD, P. M.: Radar Ambiguity Analysis. R.R.E. Technical Note No. 731, Feb. 1967.
[5] BERKOWITZ, R. S.: Modern Radar. John Wiley, 1965.
[6] MCGILLEM, C. D., e.a.: An experimental random signal radar. Proc. Nat. Electr. Conf., Vol. 23, Oct. 1967.
[7] POIRIER, J. L.: Quasi-monochromatic scattering and some possible Radar Applications. Radio Science, Vol. 3, Sept. 1968, p. 881.
[8] CRAIG, S. E., FISHBEIN, W., and RITTENBACH, O. E.: Continuous-Wave Radar with high Range Resolution and unambiguous Velocity Determination. I.R.E. Trans. MIL-6, April 1962, p. 153.
[9] CARPENTIER, M. H.: Using random Functions in Radar Applications. 'De Ingenieur', nr. 46, Nov. 13, 1970. p. E 166.
[10] GOLDBOHM, E.: De Meting van Eigenschappen van Microgolf-antennes. Tijdschrift van het NERG, Vol. 28, 1963, nr. 1-2, p. 41.
[11] SMIT, J. A.: An analogue Microwave Envelope Correlator. Christ. Huygenslab. Rep., Dec. 1964.
[12] SMIT, J. A., and KNEEFEL, W. B. S. M.: Noise-radar Experiment. Christ. Huygenslab. Rep., Jan. 1965.
[13] GABOR, D.: Theory of Communication. J. Inst. E.E. (London) Pt. III. Vol. 93, 1946, p. 429.
[14] RIHACZEK, A. W.: Principles of high-resolution Radar. Mc-Graw-Hill, 1969.
[15] SMIT, J. A.: Signalform and Resolution. Christ. Huygenslab. Rep., Dec. 1965.

Varia

Wijziging bestuur Dr. Ir. de Groot Fonds

Ir. F. de Fremery en jhr dr. ir. C. Th. F. van der Wyck traden op 4 mei 1971 uit het Bestuur van de Stichting Dr. Ir. C. J. de Groot Fonds. Het Bestuur is thans als volgt samengesteld:
Prof. ir. M. P. Breedveld, voorzitter;
Ir. W. Lulofs, commissaris;
Ir. J. D. Zijp, secretaris-penningmeester.

De secretaris, ir. J. D. Zijp.

Korte technische berichten

Elektronische beeldoverdracht als hulpmiddel bij onderwijs aan blinden

De Zweedse maatschappij Saab-Scania AB heeft een nieuw type onderwijshulpmiddel voor blinden ontwikkeld, waarmee het mogelijk is om tekeningen of diagrammen, die door de onderwijzer op een paneel zijn geplaatst, in reliëf naar een afleesscherm over te brengen dat onder bereik is van de leerling.

Deze elektronische beeldoverbrenger bestaat uit drie delen: Het eerste deel (een tekenpaneel) is toegerust met een tekenarm op een metalen stijl. Een draaibaar orgaan met pal maakt het mogelijk dat de onderwijzer de tekenarm over het gehele paneel kan bewegen.

Het tweede deel is een afleespaneel; over het oppervlak van dit paneel wordt een stevig vel papier gespannen. Bij het binnenkomen van de elektrische signalen van het tekenpaneel gaat een reliëfpen onder het vlak van het tekenpapier d.m.v. een reeks tikken de tekening reproduceren.

Een vooraf opgenomen commentaar kan via het derde deel, een gesynchroniseerde bandspeler, als begeleidende toelichting ten gehore worden gebracht.

Wanneer een bepaald beeld is overgebracht kan de blinde leerling op eenvoudige wijze het papier wegnemen om het later nog eens te kunnen aftasten. Een nieuw vel kan dan worden opgespannen.

De onderwijzer kan ook direct zijn commentaar bij het overbrengen van de tekening geven. Oponthoud en irritatie bij de leerling, vaak veroorzaakt bij gebruik van conventionele (tevoren gemaakte) reliëftekeningen, zullen bij het toepassen van dit systeem kunnen worden vermeden.

Het Zweedse Instituut voor Gehandicapten en de Zweedse Vereniging van Blinden gaven hun medewerking aan dit project.

SIP, Swedish International Pressbureau.

Radarbaken voor de zeevaart op lichtplatform

De Dienst van het Loodswezen zal in de tweede helft van 1971 een radar-navigatiebaken installeren op een nieuw lichtplatform, dat het lichtschip Goeree gaat vervangen. Het lichtplatform zal in de Noordzee worden geplaatst bij de ingang van de Nieuwe Waterweg. Het platform (compleet met werkplaatsen, motorkamer, helikopter-dek en vuurtoren) zal op een vierpuntsfundering in de zeebodem worden verankerd. Op het lichtplatform komt een vuurtorenlicht met een sterkte van 2,5 miljoen kaars, bij normaal weer zichtbaar tot op 16 mijl.

De radarbakenuitrusting ('racon'), bekend onder de naam '*Sea Watch*' *Major*, wordt geleverd door Ships Radio Service te Schiedam en gefabriceerd door: Associated Electrical Industries Ltd. in Engeland. Het baken werkt in de zgn. X-band (9300-9500 MHz); het geeft, bij ontvangst van de radarsignalen van een schip dat zich in de omgeving ophoudt, een identiteitscode ter lengte van circa 10 μs af. De antenne van het baken bestaat uit een vaste verticale golfpijp, voorzien van gleufstralers, waardoor het geheel als een horizontale rondstraler fungeert. Via een striplijncirculator is de antenne met de ontvanger en de zender van het baken verbonden. Aan de ingang bezit de ontvanger een 'hot-carrier' diode detector, welke wordt gevolgd door een videoversterker.

De zender zendt zijn identiteitscode uit wanneer op de ontvangeringang een radarsignaal van meer dan −66 dBW binnenkomt. De zenderoscillator wordt continu door een zaagtandgenerator verstemd, waardoor de frequentie van de zender in 72 s de band van 9300 tot 9500 MHz doorloopt Het pulsvermogen bedraagt 300 MW.

De antenne wordt beschermd door een perspex radome van 9,5 mm dikte en 20 cm doorsnede. Het baken heeft een totale hoogte van 74 cm; indien voldoende hoog geplaatst, verkrijgt het baken een reikwijdte van 20 km.

Nederlandsche Standard Electric Maatschappij N.V.